Journal of Cultural Heritage 42 (2020) 64–71

Available online at
ScienceDirect
www.sciencedirect.com

Elsevier Masson France
EM|consulte
www.em-consulte.com/en

Original article

Colorimetric and spectral data analysis of consolidants used for preservation of medieval plasterwork

Miguel Ángel Martínez [a,*], Ana Isabel Calero [b], Eva María Valero [a]

[a] Color Imaging Laboratory, Department of Optics, University of Granada, Faculty of Sciences, Campus Fuentenueva s/n, 18071 Granada, Spain
[b] Department of Painting, University of Granada, Faculty of Art, 18071 Granada, Spain

ARTICLE INFO

Article history:
Received 10 May 2019
Accepted 28 August 2019
Available online 7 September 2019

Keywords:
Restoration
Consolidation
Plasterwork
Spectral imaging

ABSTRACT

The incorporation of new methods of heritage analysis belonging to other branches of science is currently providing very useful tools for the examination of preservation products. This paper outlines the use of spectral images as an alternative to traditional colorimetry measurements carried out with a spectrophotometer for the evaluation of color changes produced by consolidation treatments applied on polychromed plasterwork. Thus, for this investigation we used a total of 18 plaster test specimens which reproduce the techniques and materials present in plasterwork from the medieval era, on which a selection of six currently-used consolidants was applied. By doing this, we have proved that the use of this method over traditional colorimetry has several advantages, such as the analysis of spatial homogeneity or obtaining colorimetric data of the entire scanned surface.

1. Introduction

One of the most important preservation problems that medieval plasterwork still presents nowadays is the discohesion of the polychrome decorations which, if not treated promptly, quite often leads to the loss of the original appearance. In some monuments, such as the Alhambra of Granada or the Royal Alcazar of Seville, or in archaeological museums, it is common to see how little color remains in these sorts of coatings [1–3]. This loss has occurred as a result of various factors. The main factor is humidity since these decorations are generally found outdoors. In these conditions, the plaster base material and the polychromies are continuously exposed to uncontrolled humidity and temperature fluctuations. This leads to alterations amongst which we can highlight the crystallization of salts in the plaster, condensation, gum denaturation or pigments alteration. Together with this issue, it is important to mention as well the harmful action of the application of subsequent superposed layers over the original plasterwork, either as a whitewashed or as a repainting. The former were aiming to hide the original polychromy in order to adopt more classicist aesthetics, or as a restructuration. The latter were aiming to highlight the lost colors due to degradation, or to change them due to new trends in aesthetics. The problem here is that these actions were usually carried out with oils and resins forming a waterproof layer which avoids the perspiration of the underlying materials, accelerating thus their degradation. Moreover, harsh cleansing over the years performed with inadequate materials and not following the current restoration criteria, has also contributed to the degradation and loss of the original color of this type of decorations. All these factors lead to our knowledge being very scarce about what the original color of these decorations was. (Fig. 1).

Thus, even though there are numerous studies regarding these sorts of decorations, most of them focus either on typological or historical matters and there are very few on specific treatments for the preservation of the original color [4–6]. Studies and publications related to the preservation of plasterwork are limited, although it seems the interest in researching these kinds of consolidants as well as their behavior in plaster is growing. However, so far interest has generally focused on the effectiveness on the base material [7]. Prominent amongst these studies are the ones carried out by the preservation laboratory of the Alhambra [8], which has focused its feasibility studies on the base material response to the application of these treatments against humidity (optic and tactile examination, adsorption tests, desorption test and humidity-dryness cycles). The results of these studies are relevant and have been taken into consideration for this paper, yet they fail to address the effect of these treatments on the color of pictorial layers [9]. Some authors have already drawn attention to the changes produced on color layers by these kinds of treatments, namely, Luigi Borgioli and Cremonesi, who state that it is essential to analyze the changes produced by these products on the optic features of the artwork,

* Corresponding author.
E-mail address: martinezm@ugr.es (M.Á. Martínez).

https://doi.org/10.1016/j.culher.2019.08.010
1296-2074/

Fig. 1. Polychrome residues in medieval plasterwork. Left: royal chamber of Santo Domingo, Granada. Center: the oratory in the Madrasa, Granada. Right: royal Alcazar of Seville.

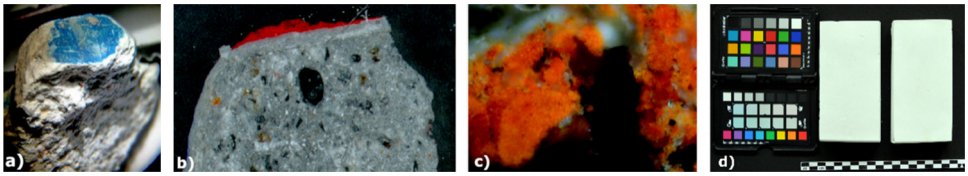

Fig. 2. Identification of the original polychromy in samples extracted from the plasterwork of the Courtyard of the Maidens in the Royal Alcazar of Seville. a: stereoscopic microscope image of natural azurite; b: optical microscopy image of lead cinnabar; c: optical microscopy image of lead red; d: general image of non-polychromed plaster test specimens.

as the legibility of the work is crucial when it is being restored [10].

Some authors have also recently studied the color changes in wall paintings due to the application of consolidants [11]. However they limit their study to the use of area-based measurement devices such as spectrophotometers.

2. Research aims

The aim of this study is twofold. First, to determine the best consolidant, from a colorimetric point of view, for the preservation of color in medieval plasterwork. We do so by using hyperspectral image capturing as an alternative to the color examination with a spectrophotometer used in previous heritage research [12–14]. Amongst the advantages offered by this method is the possibility of carrying out a colorimetric analysis of the entire scanned surface rather than just specific points. Besides one can access a comprehensive spatial homogeneity analysis (as explained in section 3.3) that provides information on the changes that have occurred. The second aim is to propose a hyperspectral imaging framework to study the effect of applying new treatments to this kind of samples.

The two main research goals stated before can be developed into the following secondary aims:

- describe the production of test specimens that reproduce materials and implementation techniques representative of medieval plasterwork on which colorimetric analysis can be carried out;
- make a representative selection of consolidant treatments and later apply them to the pictorial surface of the colour samples;
- to examine the repeatability of the color of the pigment samples by means of using the different pigment samples before applying the consolidant to each of them. The colorimetric and spectral differences we might find in this analysis will allow us to adopt an estimate tolerance for each pigment, based on the variability of the samples' own application process;
- to examine the effect of applying the consolidant in the spatial homogeneity and the color of the sample in order to determine whether there are consolidants that might alter the sample to a greater extent than others.

3. Material and methods

3.1. Plaster probes

For this study, we used plaster test specimens that reproduce the original technique of medieval plasterwork. In order to determine the technique and material used, we took into account previous research on these types of coatings [9,15]. We also took into account other studies conducted by our team on heritage works of a similar age, particularly the Royal Chamber of Santo Domingo [16], the oratory in the Madrasa [17] in the city of Granada and the plasterwork in the Royal Alcazar of Seville. Thus, we made a total of 18 test specimens (Fig. 2d), each with an area of 6.5 × 13 cm and a thickness of 1.5 cm. They were positioned in consecutive sheets from which specimens of the desired size were subsequently removed. For the supports we decided to use semi-hydrated or hydrated plaster ($Ca\ SO_4 \cdot 1/2H_2O$) as the main component as it appears in this type of decoration, to which a certain amount of calcium hydroxide was added ($Ca\ OH_2$) 5%, which has generally been used in these decorations as setting retardant.

For the polychromy of the test specimens we selected three pigments (Fig. 2a–c) which have been frequently identified in these decorations (azurite [AZ, Ref K.10200], cinnabar [CN, Ref, K.42000] and lead red [LR, Ref, K.42500] manufactured by Kremer Pigmente [18]), and we decided to use animal glue as a binder (rabbit-skin glue manufactured by CTS [19]) since it is one of the most commonly used in these types of decorations. In order to facilitate the application of the polychromy as well as the homogeneity of the samples we applied the first layer using only animal glue, followed by two consecutive layers of pigment and binder with a soft bristle brush (as can be seen in Fig. 3).

3.2. Consolidants

To help us decide on the types of consolidants to use we examined the available bibliography on interventions carried out on these types of coatings. We chose six consolidants including the ones used traditionally as well as the most recently incorporated to the market.

The products we chose for this test were ethyl silicate (Estel 1200, BE), ethyl silicate (Nanoestel, NE), acrylic resin (Paraloid® B72, PAB72), hydroxypropyl cellulose (Klucel®G, KL), polyvinyl butyral (Mowital® B60H, MW) and thermoplastic polymer (Aquazol®, AQ). Thus, six plaster probes were made, on which

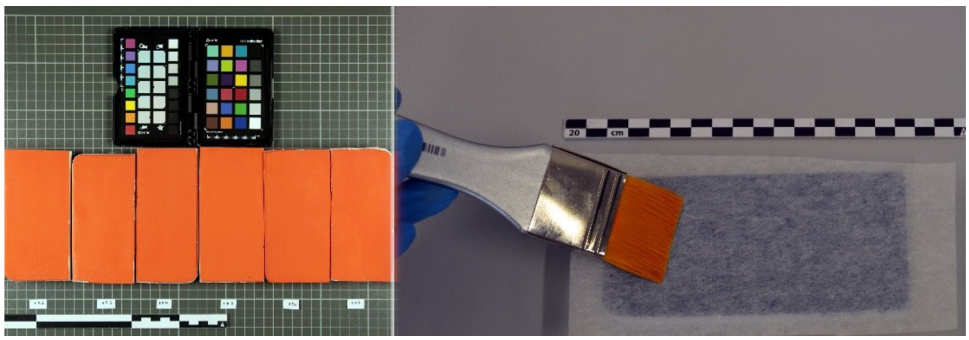

Fig. 3. Left: LR test probes. Right: application of binder.

Table 1
Chemical composition, commercial brand names and preparation procedures of the six consolidants applied on the polychrome layers of the test specimens.

Name	Consolidant	Trade name	Preparation
BE	Silicic acid ethers modified with preservers	Bioestel 1200 (CTS)	Undiluted
NE	Nano dimensions Silicon dioxide	Nanoestel (CTS)	Concentration: 1 nanoestel/3 distilled water
PAB72	Acrylic Copolymer (Ethylmethacrylate/methylacrylate, EMA/MA)	Paraloid® B72 (CTS)	TACO8 (45%, 32% y 23%, isopropyl alcohol, octane and acetone) solution 5%
KL	Hydroxypropylcellulose	KLUCEL® G (CTS)	1% in a solution (20% water and 80% ethanol)
MW	Polyvinyl butyral	Mowital® B60H (CTS)	Ethanol solution/5%
AQ	Thermoplastic polymers made of poli (2-ethyl-2-oxazoline)	AQUAZOL® (CTS)	Distilled water solution/5%

the pigments and binder, and afterwards the above-mentioned products were applied. As to the method, each product was applied by means of impregnation, using a brush on the pictorial surface and following the preparation procedures detailed in Table 1.

3.3. Colorimetric and spectral analysis method

The recording system used for obtaining the spectral image data was a hyperspectral camera Pika L (Resonon Inc., Canada). This line-scan camera allows the capture of spectral information of the samples (in our particular case, spectral reflectance). Its operating spectral range is from 380 up to 1080 nm. Its sampling interval is of approximately 4 nm after applying the hardware spectral binning technique to increase the signal to noise ratio within the capture. The lighting used was halogen (incorporated to the recording system), and the white sample used as reference was a calibrated Teflon plate. The recording system also incorporates dark signal correction as part of the image processing before obtaining the reflectance data for each spectral image. To adjust the focus position, we used the central area of the visible spectrum as reference (i.e. 550 nm). The exposure time was fixed using the white reference.

We analyzed both the spatial homogeneity as well as the colorimetric and spectral information based on both the total amount of captured data and the average spectral reflectance of such data. In this article, the spatial homogeneity is calculated as the band-wise standard deviation of the spectral image values. Other authors have used a similar approach in previous studies related to a different application field [20]. Our approach is based only in a first-order statistical parameter (the standard deviation), as described within the framework of first-order statistical texture metrics in [21]. This method does not make use of the specific spatial coordinates of the pixels for the calculation, as it is typically done when computing texture metrics based on Grey Level Co-occurrence matrices (GLCM, [22]). However, information from different spatial locations throughout the entire studied area is compared. This analysis is simpler and faster than, for instance, GLCM-based texture analysis, in which more spatially-related parameters are included in the calculations (such as spatial coordinates, orientations, etc.). Yet it suffices to adequately describe the sample variations that are of interest for the application presented in this study.

We extracted an area of roughly uniform appearance from each complete sample, sized 224 × 224 pixels. We used the 50,176 spectral reflectance vectors of the selected area for the spectral and colorimetric analysis. Afterwards we calculated the colorimetric data for each vector and then we computed the standard deviation from the full set of reflectance vectors, for each wavelength. The standard deviation data were used to estimate the degree of spatial homogeneity of the samples, which might be altered if the consolidants are applied.

The color space we chose for the graphic representation of the samples was CIELAB [23] under D65 illuminant. The spectral range used was from 400 to 700 nm. Spatial homogeneity was also studied by analyzing the color coordinate distributions obtained by computing the L*, a*, b* values for each reflectance vector, as the most homogeneous samples tend to present smaller distributions (point clouds) in the L*, a*, b* color space.

We also determined the average spectral reflectance of each sample, by computing the mean of the reflectance values of the 50,176 pixels for each spectral band. This average reflectance would be similar to the reflectance obtained with a conventional spectrophotometer that measured a similarly sized (224 × 224 pixels) spatial area. Since this device operates by integrating the light received from the measurement area, the reflectance obtained can be assumed to be very close to the average reflectance that we have computed from the individual pixel spectral reflectance vectors, save for the differences inherent to the measurement geometry and the instrument design.

For the average reflectances we also analyzed the differences in the colorimetric attributes L*, C* and h* (lightness, chroma and hue), which were calculated from its coordinates L*, a*, b*. These attributes are related with our color perception and thus help us understanding in which of them the main differences are found.

Table 2
Average and standard deviation (STD) for the comparisons 2 to 2 of the 6 samples for each pigment (AZ: azurite; CN: Cinnabar and LR: lead red) before the application of the consolidant.

Average (STD)	AZ	CN	LR
CIEDE2000	1.1582 (0.6224)	0.2740 (0.1153)	0.4662 (0.2316)
cGFC	0.00015 (0.00012)	0.000031 (0.000029)	0.000029 (0.000030)
RMSE	0.0035 (0.0014)	0.0064 (0.0042)	0.0082 (0.0038)

In order to determine the differences between samples from the obtained average reflectance data, we used a set of three metrics: one colorimetric and two spectral (based on the reflectance curves). The metric for color differences is the standard one recommended by CIE, CIEDE2000 [24]. The two spectral metrics are Root-Mean-Square-Error (RMSE) and complement of the Goodness-of-Fit coefficient (cGFC) [25], defined as shown in the equations (1) and (2) respectively, where n is the number of wavelengths, λ_j is the j^{th} wavelength, and R_a and R_b are the two reflectance vectors compared.

$$RMSE = \sqrt{\frac{1}{n}\sum_{j=1}^{n}\left(R_a\left(\lambda_j\right) - R_b\left(\lambda_j\right)\right)^2} \quad (1)$$

$$cGFC = 1 - \frac{\left|\sum_{j=1}^{n} R_a\left(\lambda_j\right) \bullet R_b\left(\lambda_j\right)\right|}{\sqrt{\left|\sum_{j=1}^{n}\left[R_a\left(\lambda_j\right)\right]^2\right|} \bullet \sqrt{\left|\sum_{j=1}^{n}\left[R_b\left(\lambda_j\right)\right]^2\right|}} \quad (2)$$

The metric RMSE is more sensitive to scale differences between measurements, and cGFC is more sensitive to shape differences between spectra.

4. Experimental data and results

4.1. Repeatability of the pigments' application process

Using the CIEDE2000, RMSE and cGFC values (explained in section 3.3) computed from the average spectral reflectance of the samples, we are able to empirically set tolerance thresholds, to establish if there has been a significant alteration in the sample as a result of applying the consolidant. We consider the alteration as significant if it surpasses the inherent change due to the heterogeneities generated by the pigment and binder application process. Specifically, we will set the empirical threshold as the average plus two standard deviations of the set of comparisons between pair of samples before applying the consolidants, as described below. Assuming a gaussian distribution, this criterion leaves within the tolerance threshold around 95% of the samples. We must take into account that applying the initial binder, assuming it is not too homogeneous, might also have an effect on the estimated color differences.

We proceed now to study the changes in color and spectral reflectance that are produced by the deposition of the pigments and binder in our test samples, before the application of the consolidants. In Table 2, we present the color and spectral difference values, which are an average of all the comparisons between pairs of original samples (i.e., with pigment and binder but not consolidant). We averaged a total of 15 comparisons for each pigment (six different samples compared two by two without repetitions). We also included in Table 2 the standard deviation data for the set of 15 comparisons.

The results of Table 2 show that the most colorimetrically-homogeneous pigment (the one with the lowest CIEDE2000 color difference) is CN. LR is the second most colorimetrically-homogeneous and AZ the least homogeneous, showing average color differences which exceed the observable threshold of 1 CIEDE2000 unit, and thus would be visually perceptible [26]. The changes produced in the reflectance of the samples, evaluated by the spectral differences data, show that the main changes occur in the reflectance scale, and there are very few changes in its shape (i.e. cGFC values near to zero and with a high relative standard deviation). AZ is also the least homogeneous for the cGFC values. Despite this, the AZ is slightly more homogeneous than the other pigments in the RMSE values, which could also be related to the fact that the maximum reflectance values for AZ are lower than for the other two pigments.

With the threshold criterion described above (average plus two standard deviations), the empirical threshold for CIEDE2000 color differences for AZ is 2.4 units. For CN, the threshold is 0.5 units and, for LR, one unit.

For the spectral differences, the same criterion as before for considering the differences relevant was used. We then set the thresholds as 0.006, 0.014 and 0.016 for AZ, CN and LR, respectively in RMSE. In cGFC, the thresholds are set at 0.0004, 0.00009 and 0.00009 for the three pigments respectively.

We also studied the spatial homogeneity of the samples before the application of the consolidants. In Fig. 4, we show the standard deviation curves for all the six samples of each pigment. The curve for each analyzed sample from 1 to 6 (S1 to S6) is plotted in a different color. This gives us information about how the gray levels are distributed for each sample individually (i.e. how homogeneous the distributions of spectral values are for each spectral band in each of the six samples). It can be seen that the standard deviation values we obtained are similar for the three pigments, although slightly higher for CN, especially in the area where the reflectance of this pigment is higher. It can also be seen how the spatial homogeneity is lower for the wavelengths in the near infrared (from 800 nm). This may be caused partly because of a lower signal to noise ratio for these wavelengths, since even though the lighting source emits strongly in the infrared the spectral responsiveness of the silicon sensor of the spectral camera is rather low within this range of wavelengths.

The standard deviation average data (i.e. the mean value for each curve shown in Fig. 3, averaged as well across the six samples) are 0.0107 for AZ, 0.0162 for CN and 0.0136 for LR. In general, we can see how the samples with less of a variation in terms of spatial homogeneity amongst the different test specimens of reference are AZ and LR. The spatial homogeneity in each test specimen is not related with the color homogeneity between the different test specimens, as we may conclude if we remember that AZ was the less colorimetrically-homogeneous pigment, and CN the most colorimetrically-homogeneous one. The spatial variation across pixels in each test sample may be relatively noticeable and, at the same time, however, the average color obtained from each sample by averaging data for all pixels may be rather similar between different test specimens. This adds value to the proposed method for the study on spatial homogeneity presented in this paper.

4.2. Effect of the application of the consolidant

4.2.1. Effects on the average color and spectral reflectance of the samples

Table 3 shows the data of spectral and color differences between the average reflectances both before and after applying the consolidant to the three pigments and six consolidants studied. Results

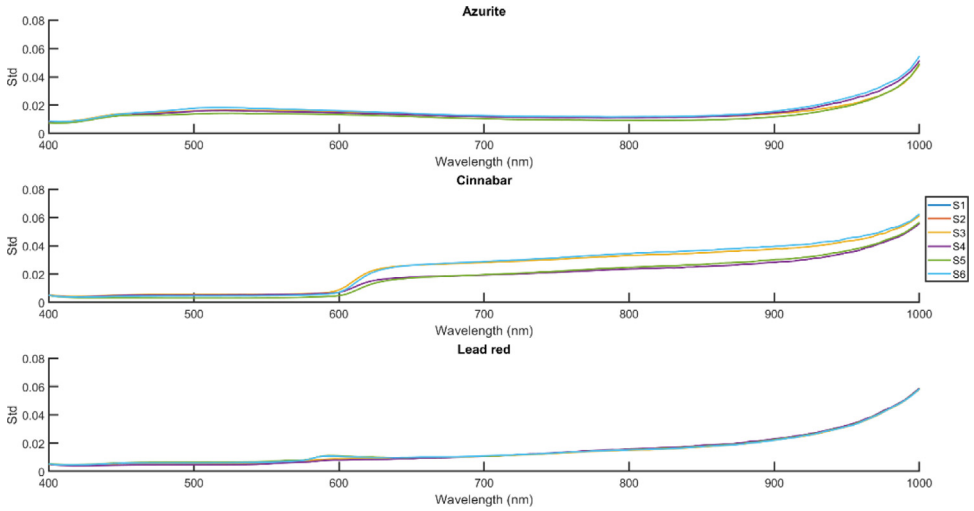

Fig. 4. Standard deviation across pixels (STD curves) as a function of wavelength for the six samples (S1 to S6) of each of the three pigments analyzed.

Table 3
Color and spectral metrics comparing the mean reflectances before and after applying the consolidant for the three pigments independently (AZ: blue; CN: orange and LR: red), and the average of the three (gray).

	Bioestel1200	Nanoestel	Paraloid® B72	Kluce® G	Mowital® B60H	Aquazol®
AZ						
CIEDE00	9.554	4.216	3.417	3.169	3.587	3.170
cGFC	0.004070	0.000113	0.000051	0.000025	0.000036	0.000144
RMSE	0.073	0.034	0.027	0.025	0.028	0.024
CN						
CIEDE00	6.865	6.608	8.349	6.154	16.217	10.684
cGFC	0.002120	0.001760	0.002935	0.001216	0.014356	0.006176
RMSE	0.066	0.066	0.082	0.068	0.167	0.097
LR						
CIEDE00	5.772	4.383	6.880	4.808	10.700	9.498
cGFC	0.001064	0.000464	0.001729	0.000626	0.005518	0.004141
RMSE	0.090	0.082	0.107	0.075	0.165	0.143
Average						
CIEDE00	7.397	5.069	6.215	4.710	10.168	7.784
cGFC	0.002418	0.000779	0.001572	0.000622	0.006637	0.003487
RMSE	0.076	0.061	0.072	0.056	0.120	0.088

show the three pigments separately (blue, orange and red color bands for AZ, CN and LR respectively), and the average of the three (gray color band in Table 3).

Regarding the average differences (gray section in Table 3), we found that the differences caused after applying the consolidants surpass the empirical thresholds set in section 4.1, and thus can be considered as higher than the color variations inherent to the pigment and binder deposit procedures. The consolidant which most altered the color of the sample was Mowital®B60H, followed by Aquazol® and Bioestel1200. The consolidant which least altered the color of the sample was Klucel® G, followed by Nanoestel.

Regarding the spectral metrics, we also found that the changes induced by the application of the consolidant are above the empirical thresholds set in section 4.1. Mowital®B60H was also the consolidant that produced the highest changes in the shape of the spectral reflectance. As we can see, the cGFC values are higher than those for the rest of consolidants. This implies that the spectra are less similar in terms of shape, as two identical spectra would result in a null cGFC. This consolidant is also the one that has the highest values of RMSE. This means that, on average, it has affected the spectral reflectance of the samples to a greater extent. For the three pigments, the metric that presented the lowest relative variation was cGFC.

For AZ (blue color band in Table 3), the consolidant which caused the highest differences was Bioestel1200 followed by Nanoestel. These consolidants also seem to cause differences in terms of shape and scale in the average reflectance. The ones that least altered the color of the sample were Klucel® G and Aquazol®. For CN and LR, however, Mowital®B60H and Aquazol® were the consolidants that caused the largest number of changes in the color of the sample, and Klucel® G and Nanoestel the ones that least influenced the average color. The spectral metrics are in agreement with the results of color difference.

The global results we obtained may also be explained by considering the composition of the different consolidants used. In the case of Klucel® G, it is quite logical that this is one of the products that least changed the surface of the sample. This is because it is a very flexible product that does not contain any plasticizer. It has several advantages, for instance, it leaves no stains or marks and it is very transparent [27]. Besides, we applied the product using a very low concentration for this test, and this favored its absorption in the plaster supports. In subsequent phases of this work, we will also check the bonding strength compared to the other products we used. The feasibility of its use, which has been studied thus far in other supports, needs to be further analyzed. It should be pointed out that Paraloid®B72 presents an intermediate behavior in the treated samples, and was not, in any of the cases, one of the products that most changed the color of the sample. These results therefore agree with previous colorimetric studies [9,28,29]. However, it is worth mentioning that this product presents some

Table 4
Variation in chromatic attributes L*, C* and h* when applying the consolidant for the three pigments AZ, CN and LR.

	Bioestel1200	Nanoestel	Paraloid® B72	Klucel® G	Mowital® B60H	Aquazol®
AZ						
ΔL*	9.879	4.536	3.708	3.470	3.937	3.482
ΔC*	−2.632	1.093	0.765	0.792	0.780	0.097
ΔH*	0.530	−1.087	1.132	−0.099	0.030	0.010
CN						
ΔL*	6.377	6.285	7.937	5.984	15.793	9.956
ΔC*	−6.037	−4.838	−6.696	−3.399	−15.009	−10.423
Δh*	−3.415	−2.778	−3.051	−2.107	−5.325	−4.216
LR						
ΔL*	5.651	5.093	7.050	4.478	10.598	9.168
ΔC*	−8.004	−3.191	−9.729	−6.186	−17.523	−15.479
Δh*	−3.966	−1.629	−4.179	−3.614	−7.317	−6.791
Average						
ΔL*	7.302	5.305	6.232	4.644	10.110	7.535
ΔC*	−5.558	−2.312	−5.220	−2.931	−10.584	−8.602
Δh*	−2.283	−1.831	−2.033	−1.940	−4.204	−3.665

In all cases, we took into account the attribute before the apply as the reference (e.g. ΔL* = L*after – L*before).

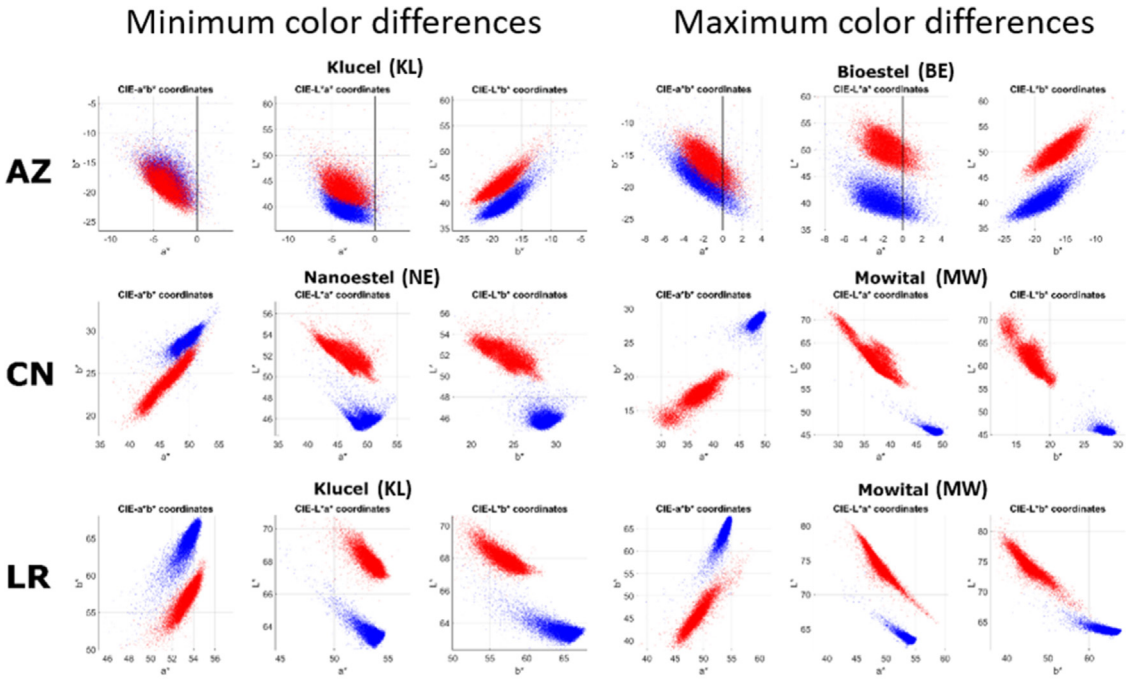

Fig. 5. L*a*b* plots for the minimum color difference (left three columns) and maximum color difference (right three columns). Data for AZ (first row), CN (second row) and LR (third row). Blue before the consolidant application and red: after. Please note the different scales used in some cases on the plots of the right and left groups.

disadvantages when applied, especially in wet environments and at high concentrations, since the resin tends to reticulate, and then it may lose reversibility, reduce permeability and may also produce opacity.

We may also consider as positive results those obtained when we globally analyzed the samples treated with ethyl esters (Nanoestel especially). This product is highly compatible with the treated substrate, which would make it a suitable product for the treatment of these decorations and whose effectiveness in plaster supports has already been evidenced in other studies [28]. As for the Bioestel1200, it seems to produce relatively high differences in color and spectral metrics for the AZ pigment.

As to the consolidant Aquazol®, we can see that it does produce remarkable changes in terms of color. Despite it being a product that presents good reversibility and ageing resistance, there is a chance that, as happens with other resins, the product may have a low penetrating power, which would make it to stay on the surface forming a film and then it may produce some very noticeable changes in appearance [30]. Finally, we want to emphasize that the data we obtained by applying the polyvinyl butyral (Mowital®B60H) are strictly related to its chemical composition. This product, once applied to the surface, provides a consistent and thermoplastic film that may be the reason for the above-mentioned color differences compared to other types of treatments, such as those based on silicon esters (Nanoestel, Bioestel1200) or hydroxypropylcellulose (Klucel® G).

Having analyzed the variation of the chromatic attributes (shown in Table 4), we inferred that the global variation tendencies of the attributes for chroma and hue differed between AZ and the two red pigments, although they did not differ for the variation in lightness: the consolidant tended to generally lighten the samples (positive variations for L*). In the case of chroma, the consolidant tended to generally make the sample less vivid for red, especially for LR, whereas for AZ this tendency only occurred with BE. As to the hue, there is a positive, smaller angle rotation for AZ, and a negative, larger one for the red pigments. This implies that

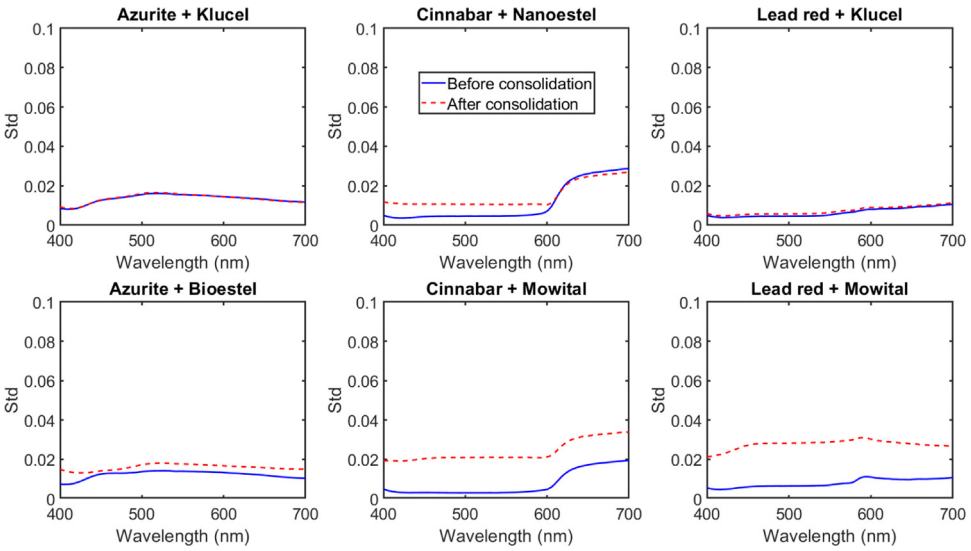

Fig. 6. STD plots for the minimum color difference (upper row) and maximum color difference (lower row). Data for AZ (left column), CN (middle column) and LR (right column). Blue: before the consolidant application and red: after.

the hue angle increases very slightly for AZ, whilst it decreases for CN and LR (they would change from a more orange hue to a redder hue). Out of the three analyzed variations, on average, the biggest change occurred in terms of lightness, except for Mowital®B60H and Aquazol®, which produced greater variations in chroma in terms of magnitude.

4.2.2. Effects on the color distributions of the samples and their color spatial homogeneity

The consolidants which produced maximum and minimum color differences for each pigment were identified using the data in Table 3. For those two consolidants, we show in Fig. 5 the distributions of L*, a*, b* values. Each point of these data clouds corresponds to one pixel in the images. The differences shown in Table 3 are computed from the mean color of these distributions, obtained from the average reflectance data.

The L*, a*, b* clouds of Fig. 5 allow us to further analyze the color variation of the test specimens when adding the consolidant, and also the homogeneity of the color of the samples before the application of the consolidants. For AZ, we can see that both for KL (minimum difference in average color) and BE (maximum difference in color), the major variation is produced in the lightness of the samples, rather than in the chroma, according to what is shown in Table 4. But we can also notice that the area of the clouds for this pigment (which is related to the spatial homogeneity of color in the studied test specimen) is very similar before and after the application of the consolidant. This goes to show that we mainly found that both KL and BE lightened the sample, but they did not make it less homogeneous in terms of color, although BE did introduce some changes in the hue, increasing the value of b*.

For CN and LR, the application of the consolidant produced a clear change in the chroma of the sample, as well as a modification of the lightness and, to a lesser extent, the hue. Furthermore, we can see that there is a clear change for MW and NE in terms of the size of the color clouds, which increased within the test specimens when the consolidant was applied. This indicates that the consolidant provokes a loss of spatial homogeneity in the color of the sample, widening the cloud in the three dimensions of the color clouds (L*, a* and b*). This change is, logically, much more extreme in the case of MW, which resulted in the highest difference in average color of the sample.

As to the spatial homogeneity of the samples before applying the consolidant, we can notice how the color clouds are much more elongated for CN and LR than for AZ. This tells us that for red pigments the color tends to a greater extent to be distributed in a predictable way. In other words, there is a higher correlation between the figures for a* and b* found for CN and LR without consolidant than for AZ. The correlation coefficient values for a* vs. b* are −0.517 for AZ, 0.771 for CN and 0.861 for LR. This trend towards higher correlation for the red pigments is maintained after the application of the consolidant as well, with correlation coefficient values of −0.605 for AZ, 0.952 for CN and 0.868 for LR.

For the rest of the analyzed consolidants, the tendencies were similar to those already described.

4.2.3. Effects on the spatial homogeneity of the sample in terms of wavelength

In Fig. 6, we show the standard deviation curves for different wavelengths corresponding to the extremes in color variations analyzed in Fig. 5.

Generally speaking, except the case of CN with NE, we found a similar dependency of the spatial homogeneity with wavelength before and after the application of the consolidant. The consolidant tended to elevate the standard deviation curves for the MW, and did not cause any changes in these curves for KL. For CN once the NE had been applied, there was an increase for wavelengths below 600 nm. The data of the spectral standard deviation curves show a clear agreement with the conclusions inferred regarding spatial homogeneity when we analyzed the color distributions (Fig. 5). However, for the CN with NE applied, the spectral curves can discriminate a greater change in the area of short wavelengths, which is not clearly shown in the color distributions, as the expansion in the size of the clouds is relatively similar for coordinates a* and b*. This change is more remarkable if we take into account that the reflectance of CN is lower for short wavelengths, which leads to more reduced signal values (in general, the standard deviation is correlated to the signal level). However, for KL, the standard deviation curves did not change much, although the reflectance of the consolidated samples was slightly higher, as deduced from its higher levels of lightness.

5. Conclusions

In this study, we have proven the usefulness of hyperspectral image capture for analyzing the effect of the application of a consolidant on plaster test specimens prepared with three pigments (natural azurite, cinnabar and lead red), bound with animal glue,

which are the materials usually used in the polychrome of medieval plasterwork. The spectral imaging system allowed us to obtain data of spatial homogeneity in the area of the studied test specimen, both in terms of wavelength and using distribution of points with color clouds in a color space. It also allowed us to conduct an analysis by using the average color differences (which would be the equivalent to the data obtained using a spectrophotometer or a conventional colorimeter). The results we obtained in general terms for the three pigments indicated that the consolidant that least altered the color of the sample and introduced fewer changes in its reflectance curves was Klucel® G, whilst the one that most altered the sample was Mowital®B60H. Furthermore, the analysis derived considered the dependency of the standard deviation with wavelength and allowed us to detect a slightly higher change in the spatial homogeneity for some wavelengths in the case of NE for CN. The visualization of the color data clouds in the space L*a*b* allowed a much more complex and complete characterization than the one we might obtain from a simple analysis of the data of the average color difference. In general, we found agreement between the data of the average color difference and the tendencies shown for the spatial homogeneity, although this combined analysis also revealed some interesting data about the uniformity of the application of the pigment in each test specimen, which is slightly higher in the case of AZ, whilst the test specimens with AZ applied have a lower degree of repeatability. When analyzing data of spatial homogeneity based on spectral standard deviation, it is important to consider, however, that standard deviation depends, to a certain extent, on the signal level of the sample, as also happens with the CIEDE00 and RMSE metrics. We also analyzed the main changes found in the average chromatic attributes of the samples, which helps to better understand the modifications in the global color made by the application of the consolidant. The global results we obtained may also be explained in terms of the composition of the different consolidants used, as well as the concentrations at which they were used.

Nevertheless, the data obtained so far will be complemented in the future by means of a study of test specimens held in an ageing test chamber, after we will carry out absorption, determination of the penetration of the consolidant products and resistance to solubility tests.

Moreover, as an additional study in the future, we plan to tackle a more detailed characterization of the changes in the texture of the samples produced by the application of the consolidant. In this work, as explained in section 3.3, a simple spatial homogeneity analysis has been performed, which did not account for spatial coordinates or orientations. We plan to use an analysis of textures based on statistical parameters extracted from the Gray Level Co-occurrence matrix [22] and incorporating the analysis in different bands of the spectrum.

Funding

This work has been funded by the Ministry of Economy and Competitiveness and by the European Regional Development Fund (MINECO/ERDF, EU) within the framework of the Research Project HAR2015-66139-P, as well as by the Excellence Project of the Andalusian Regional Government P12-HUM-1941.

References

[1] O. López Cruz, A. García Bueno, V.J. Medina Flórez, Antonio, Sánchez-Navas, A methodology for timing interventions made on the polychrome decorations of the facade of the Palace of King Peter I, the Royal Alcázar of Seville, Spain, J. Cult. Herit. 20 (2016) 573–582.
[2] P. Malta da Silveira, M.R. Veiga, J. Brito, Gypsum coatings in ancient buildings, Constr. Build. Mater. 21 (1) (2007) 126–131.
[3] V. López Borges, L. Burgio, R. Clark, Documentación y autentificación de yeserías nazaríes a través del tratamiento de conservación y análisis científico. Actas del II Congreso del Grupo Español del IIC. Investigación y conservación, Universidad Politécnica de Valencia, Barcelona, 2005, pp. 109–125.
[4] A. García-Bueno, V.J. Medina-Flórez, A. González, La policromía de los fragmentos de yeso almacenados en los depósitos del Museo de la Alhambra, in: In prepint 16th International Meeting on Heritage Conservation, UP Valencia, Valencia, 2006.
[5] M.J. Domínguez Vidal, R. De la Torre-López, M.J. Rubio Domene, De la Torre Áyora-Cañada, In situ noninvasive Raman microspectroscopic investigation of polychrome plasterworks in the Alhambra, Anal. 137 (24) (2012) 5763–5769.
[6] R. Villegas Sánchez, F. Arroyo Torravlo, R. Rubio Domene, E. Correa, Sánchez, Study of efficiency and compatibility on successive applications of treatments for islamic gypsum and plaster from the Alhambra. Science and art: a future for stone, 2016, pp. 613–620.
[7] F. Jroundi, M.T. González-Muñoz, A. Garcia Bueno, C. Rodríguez-Navarro, Consolidation of archaeological gypsum plaster by bacterial biomineralization of calcium carbonate, Acta Biomater. 10 (9) (2014) 3844–3854.
[8] R.R. Domene, Yeserías de la Alhambra, Historia, Técnica y Conservación, Ed. Universidad de Granada-Patronato de la Alhambra y el Generalife, 2010.
[9] C. Cardell-Fernández, C. Navarrete-Aguilera, Pigment and plasterwork analyses of Nasrid polychromed lacework stucco in the Alhambra (GranadaSpain), Stud. Conserv. 51 (3) (2006) 161–176.
[10] L. Borgioli, P. Cremonesi, Le resine sintetiche usate nel trattamento di opere policrome. Saonara, 2005 [Il prato].
[11] J. Bagniuk, D. Białek-Kostecka, A. Forczek-Sajdak, Z. Kaszowska, J. Skrzelowska, Color changes in wall paintings under the influence of consolidation with synthetic polymers, Color Res. Appl. 44 (5) (2019) 772–782.
[12] J.S. Pozo-Antonio, C. Montojo, M.L. de Silanes, I. de Rosario, T. Rivas, In situ evaluation by colour spectrophotometry of cleaning and protective treatments in granitic cultural heritage, Int. Biodeterioration & Biodegradation. 123 (2017) 251–261.
[13] M.F. Alberghina, R. Barraco, S. Basile, M. Brai, L. Pellegrino, F. Prestileo, et al., Mosaic floors of roman Villa del Casale: principal component analysis on spectrophotometric and colorimetric data, J. Cult. Herit. 5 (1) (2014) 92–97.
[14] M. Castillejo, M. Martín, M. Oujja, J. Santamaría, D. Silva, R. Torres, et al., Evaluation of the chemical and physical changes induced by KrF laser irradiation of tempera paints, J. Cult. Herit. 4 (2003) 257–263.
[15] A. Domínguez Vidal, M.J. De la Torre-López, R. Rubio Domene, M.J. Áyora-Cañada, In situ noninvasive Raman microspectroscopic investigation plasterworks in the Alhambra 13, Anal. 137 (24) (2012) 5763–5769.
[16] A. García Bueno, V.J. Medina, Flórez, The Nasrid plasterwork at "qubba Dar al-Manjara l-kubra" in Granada: characterisation of materials and techniques, J. Cult. Herit. 5 (1) (2004) 75–89.
[17] A. García Bueno, V.J. Medina Flórez, A. González, Segura, La policromía de las yeserías del oratorio de la Madraza de Yūsuf I, Granada. Primeras aportaciones del estudio de materiales para la localización de zonas originales y añadidos, Al-Quántara 31 (2010) 245–256.
[18] https://www.kremer-pigmente.com/es.
[19] https://www.ctseurope.com/es/scheda-prodotto.php?id=2676.
[20] J.L. Riera, J.J. Magnuson, J.R.V. Castle, M.D. MacKenzie, Analysis of large-scale spatial heterogeneity in vegetation indices among North American landscapes, Ecosystems 1 (3) (1998) 268–282.
[21] L. Nanni, M. Paci, F.L.C.D. Santos, S. Brahnam, J. Hyttinen, S. Alexander, Review on texture descriptors for image classification, in: Computer vision and simulation: methods, applications and technology, Nova Publications, 2016.
[22] R.M. Haralick, K. Shanmugam, Textural features for image classification, IEEE Trans. Syst. Man Cybern. (6) (1973) 610–621.
[23] N. Ohta, A. Robertson, Colorimetry: fundamentals and applications, JohnWiley & Sons, 2006.
[24] M.R. Luo, G. Cui, B. Rigg, The development of the CIE 2000 colour-difference formula: CIEDE2000. Colour research & application: endorsed by Inter-Society Colour Council, The Colour Group (Great Britain), Canadian Society for Colour, Colour Science Association of Japan, Dutch Society for the Study of Colour, The Swedish Colour Centre Foundation, Colour Society of Australia, Centre Français de la Couleur, Color Res. Appl. 26 (5) (2001) 340–350.
[25] M.A. Martínez, E.M. Valero, J. Hernández-Andrés, J. Romero, G. Langfelder, Combining transverse field detectors and colour filter arrays to improve multispectral imaging systems, Appl. Optics. 53 (13) (2014) C14–C24.
[26] Luo M.R, Minchew C, Kenyon P, Cui G. Verification of CIEDE2000 using industrial data. AIC 2004 color and paints, interim meeting of the International Color Association, Proceedings; 2004. 97–102.
[27] P. Sedano, Espín Desde los materiales tradicionales a los nuevos materiales y métodos aplicados en la conservación de obras de arte, Arbor. 169 (668) (2001) 577–589.
[28] F.J. Collado-Montero, A.I. Calero-Castillo, M. Melgosa, V.J. Medina, Flórez, Colourimetric evaluation of pictorial coatings in conservation of plasterworks from the islamic tradition, Stud. Conserv. 64 (2) (2019) 90–100.
[29] M.A. Linares Soriano, M.B. Carrascosa Moliner, Resinas acrílicas empleadas en la elaboración de masillas para la reintegración volumétrica de materiales óseos arqueológicos: estudio colorimétrico del envejecimiento artificial acelerado ultravioleta, Arche. (10) (2015) 179–190.
[30] J. Arslanoglu, Evaluation of the use of aquazol as an adhesive in paintings conservation, WAAC Newsl. 25 (2) (2003) 12–18.